Received: 26 January 2021 | Revised: 25 March 2021 | Accepted: 2 April 2021

DOI: 10.1096/fj.202100162R

RESEARCH ARTICLE

THE FASEB JOURNAL

Mechanisms of temperature modulation in mammalian seasonal timing

Laura van Rosmalen[1] | **Jayme van Dalum**[2] | **Daniel Appenroth**[2] | **Renzo T. M. Roodenrijs**[1] | **Lauren de Wit**[1] | **David G. Hazlerigg**[2] | **Roelof A. Hut**[1]

[1]Chronobiology Unit, Groningen Institute for Evolutionary Life Sciences, University of Groningen, Groningen, The Netherlands

[2]Arctic Seasonal Timekeeping initiative (ASTI), Department of Arctic and Marine Biology, UiT The Arctic University of Norway, Tromsø, Norway

Correspondence
Laura van Rosmalen, Chronobiology Unit, Groningen Institute for Evolutionary Life Sciences, University of Groningen, Building 5171, Room 0344, Nijenborgh 7, 9747 AG Groningen, The Netherlands.
Email: Lauravanrosmalen@hotmail.com

Funding information
Rijksuniversiteit Groningen (University of Groningen), Grant/Award Number: B050216; Universitetet i Tromsø (UiT)

Abstract

Global warming is predicted to have major effects on the annual time windows during which species may successfully reproduce. At the organismal level, climatic shifts engage with the control mechanism for reproductive seasonality. In mammals, laboratory studies on neuroendocrine mechanism emphasize photoperiod as a predictive cue, but this is based on a restricted group of species. In contrast, field-oriented comparative analyses demonstrate that proximate bioenergetic effects on the reproductive axis are a major determinant of seasonal reproductive timing. The interaction between proximate energetic and predictive photoperiodic cues is neglected. Here, we focused on photoperiodic modulation of postnatal reproductive development in common voles (*Microtus arvalis*), a herbivorous species in which a plastic timing of breeding is well documented. We demonstrate that temperature-dependent modulation of photoperiodic responses manifest in the thyrotrophin-sensitive tanycytes of the mediobasal hypothalamus. Here, the photoperiod-dependent expression of type 2 deiodinase expression, associated with the summer phenotype was enhanced by 21°C, whereas the photoperiod-dependent expression of type 3 deiodinase expression, associated with the winter phenotype, was enhanced by 10°C in spring voles. Increased levels of testosterone were found at 21°C, whereas somatic and gonadal growth were oppositely affected by temperature. The magnitude of these temperature effects was similar in voles photoperiodical programmed for accelerated maturation (ie, born early in the breeding season) and in voles photoperiodical programmed for delayed maturation (ie, born late in the breeding season). The melatonin-sensitive pars tuberalis was relatively insensitive to temperature. These data define a mechanistic hierarchy for the integration of predictive temporal cues and proximate thermoenergetic effects in mammalian reproduction.

Abbreviations: CP, critical photoperiod; *Dio2*, iodothyronine deiodines 2; *Dio3*, iodothyronine deiodines 3; GnRH, gonadotropin-releasing hormone; LP, long photoperiod; PNES, photoperiodic neuroendocrine system; PP, photoperiod; SP, short photoperiod; T_3, triiodothyronine; *Tshβ*, thyroid-stimulating hormone β-subunit; *Tshr*, thyroid-stimulating hormone receptor.

This is an open access article under the terms of the Creative Commons Attribution-NonCommercial-NoDerivs License, which permits use and distribution in any medium, provided the original work is properly cited, the use is non-commercial and no modifications or adaptations are made.
© 2021 The Authors. *The FASEB Journal* published by Wiley Periodicals LLC on behalf of Federation of American Societies for Experimental Biology

KEYWORDS
ambient temperature, maternal photoperiodic programming, *Microtus arvalis*, photoperiodic neuroendocrine system, seasonal reproduction

1 | INTRODUCTION

Seasonal variation in environmental cues needs to be anticipated by organisms, which is essential for survival and efficient reproduction. In species occurring in temperate climatic zones, there is a high selection pressure on timing of reproduction, causing evolution of intrinsic annual timing mechanisms that accurately time physiology, morphology, and (reproductive) behavior. The reproductive potential of short-lived rodents, such as voles, often depend on rapid postnatal reproductive development leading to multiple generations of progeny within a single breeding season.[1-3] At the end of the breeding season, however, there is a necessary shift in emphasis from breeding to overwintering survival, and pups born late in summer may delay reproductive development until the following spring. Many organisms use photoperiod as a predictor of expected seasonal changes in food and climatic conditions. Studies in several species indicate that rates of reproductive development are set in utero through transplacental relay of maternal photoperiod: gestation on a short photoperiod favors accelerated postnatal reproductive development on an intermediate photoperiod, whereas gestation on a long photoperiod favors a slow rate of postnatal reproductive development on an intermediate photoperiod,[4-11] a concept named "maternal photoperiodic programming" (MPP).[12,13] Recently, we demonstrated that this phenomenon of maternal photoperiodic programming operates in species where photoperiodic cueing is the dominant mechanism for seasonal synchronization (Djungarian hamster).[11] Bronson proposed a theoretical model,[14,15] which emphasizes short life-span (ie, small mammals; short reproductive cycle) as predisposing animals to opportunistic breeding, whereas longer lifespan (ie, ungulates, hibernators; long reproductive cycle) predisposes animals to use photoperiodic cuing. This model suggests that the latter group is more vulnerable to climate change, as a shift to higher latitudes due to global warming requires a new critical photoperiod or elimination of photoperiodic responsiveness. On the other hand, short-lived mammalian species may override photoperiodic control by using an opportunistic strategy controlled by demands that compete with reproduction such as foraging conditions, temperature and food availability. Such species may therefore be less vulnerable to climate change as they may quickly adapt to temperature changes.

This led us to ask how photoperiod and temperature interact to shape postnatal reproductive development in microtine rodents noted for opportunistic breeding patterns in which nutrient supply and ambient temperature are significant modifiers of reproductive activation.[16-23] In addressing this question we aim to create a better understanding of the neurobiological basis for temperature-photoperiod interactions driving the mammalian reproductive system.[24,25]

In vertebrates, a conserved photoperiodic neuroendocrine response system measures photoperiod and subsequently drives annual rhythms in reproduction.[26,27] Light is perceived by photoreceptors located in the retina that signal to the suprachiasmatic nucleus (SCN). The SCN projects to the pineal gland, producing melatonin during darkness.[28] As a result, daylength is encoded in the duration of nocturnal melatonin secretion. Melatonin binds to its receptor (MTNR1A, MT1) in the pars tuberalis (PT) of the anterior lobe of the pituitary gland.[29-32] For that reason, the pars tuberalis is presumably the master regulator for seasonal rhythms in mammals.[33] Under long photoperiods, pineal melatonin is released for a short duration, which stimulates thyroid-stimulating hormone β-subunit (TSHβ) production in the pars tuberalis. TSHβ forms an active dimer with glycoprotein hormone alpha-subunit (α-GSU),[34] and binds to TSH receptors (TSHr) in the tanycytes around the third ventricle. Consequently, the tanycytes increase iodothyronine deiodines 2 (DIO2) production, whereas iodothyronine deiodines 3 (DIO3) is decreased, leading to higher levels of the active form of thyroid hormone (T_3) and lower levels of inactive forms (T_4 and rT_3) in the mediobasal hypothalamus (MBH). T_3 signals possibly "indirectly," through KNDy (kisspeptin/neurokinin B/Dynorphin) neurons of the arcuate nucleus (ARC) on gonadotropin-releasing hormone (GnRH) neurons in the hypothalamus.[35] GnRH neurons project to the pituitary inducing gonadotropin release, which stimulates gonadal growth and subsequently sex steroid production. The neuroanatomy, genes, and promotor elements that are crucial in this response pathway, have been identified in several mammalian and bird species,[30,36-43] including the common vole, *Microtus arvalis*.[44,45] Recently, Sáenz de Miera and colleagues demonstrated that the *Tsh-Dio2/Dio3* system is subjected to photoperiodic regulation in utero, before the fetal pineal gland starts to produce a rhythmic melatonin signal, indicating that early life maternal photoperiodic programming operates through this pathway.[11]

To explore the levels at which photoperiodic history and thermal cues are integrated in the photoperiodic neuroendocrine system (PNES), we manipulated photoperiodic history, postweaning photoperiod and ambient temperature in captive reared common voles (*M. arvalis*, Pallas 1778), a species in which flexible timing of reproduction is extensively

documented, and assessed gonadal and somatic development alongside hormone levels and hypothalamic gene expression. Here we present the results of a systematic analysis of the impact of ambient temperature on reproductive development and postnatal photoperiodic sensitivity in winter- and summer-born pups.

2 | MATERIALS AND METHODS

2.1 | Animals and experimental procedures

All experimental procedures were carried out according to the guidelines of the animal welfare body (IvD) of the University of Groningen conform to Directive 2010/63/EU and approved by the CCD (Centrale Commissie Dierproeven) of the Netherlands (CCD license number: AVD1050020171566). Common voles (*M. arvalis*) were obtained from the Lauwersmeer area, the Netherlands (53° 24′ N, 6° 16′ E).[46] The population has been kept in the laboratory as an outbred colony at the University of Groningen, which provided all animals used in this study. Adult and weaned voles were individually housed in transparent plastic cages (15 × 40 × 24 cm) provided with sawdust, dried hay, an opaque PVC tube, and ad libitum water and food (Standard rodent chow; Altromin #141005). The experiments were carried out in temperature-controlled chambers in which ambient temperature and photoperiod was manipulated as described below.

The voles used in the experiment (134 males) were gestated and born at 21°C under either a short photoperiod (SP, 8 hours of light/24 hours: born early in the breeding season) or a long photoperiod (LP, 16 hours of light/24 hours: born late in the breeding season) and weaned at 21 days. After weaning, voles were transferred to either 10°C or 21°C and a range of different photoperiods, a laboratory equivalent to different seasonal conditions (Figure 1). Postweaning photoperiods were (hours light: hours dark): 18L:6D, 16L:8D, 14L:10D, 12L:12D, 10L:14D, 8L:16D, and 6L:18D. Physiological data from 8L:16D was published elsewhere,[45] and was only applied in the winter-born group. While all postweaning photoperiods were applied at 21°C, the extreme photoperiods were omitted at 10°C for experimental efficiency (Figure 1). All voles were weighed when 7, 15, 21, 30, 42, and 50 days old.

2.2 | Tissue collections

Voles were sacrificed by decapitation, with prior CO_2 sedation, 17 ± 1 hours after lights OFF, when 50 days old. After decapitation, trunk blood was collected directly from the vole. Blood samples were left on ice until centrifugation (10 minutes, 2600G, 4°C). Plasma was transferred to a clean tube and stored at −80°C until hormonal assay. Whole brains were carefully dissected to include the proximate pituitary stalk including the pars tuberalis. Within 5 minutes after decapitation, brains were slowly frozen on a brass block surrounded by liquid N_2. Brains were stored at −80°C until proceed to in situ hybridization. Reproductive organs were dissected, cleaned of fat, and wet masses of paired testis weight were measured (±0.0001 g).

2.3 | In situ hybridization

A detailed description of the in situ hybridization protocol can be found elsewhere.[47,48] In short, 20 µm coronal brain sections were cut on a cryostat in caudal to rostral direction, starting from the mammillary bodies to the optic chiasm, to cover the area of the hypothalamus and third ventricle. Sections were mounted onto precoated Superfrost Plus slides (Thermo scientific: ref J1800AMNZ) with 6-10 sections per slide and 10 slides per individual. Antisense riboprobes of rat *Tshβ* (GenBank accession No. M10902, nucleotide position 47-412), vole *Dio2* (GenBank accession No. JF274709, position 1-775), and vole *Dio3* (GenBank accession no. JF274710, position 47-412) were

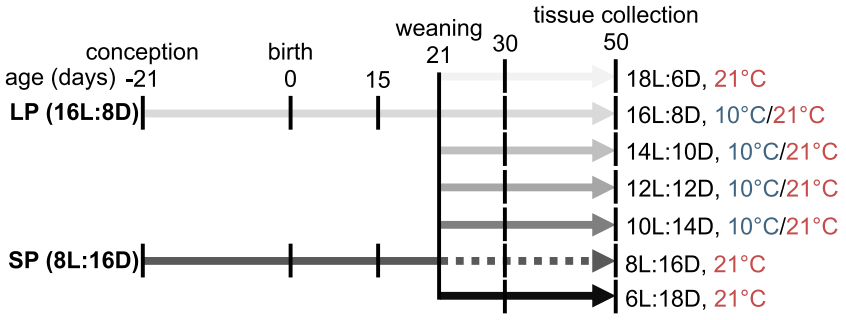

FIGURE 1 Experimental design. Conception, gestation, birth, and lactation took place under either LP (ie, summer-born) or SP (ie, winter-born) at 21°C. At the day of weaning (21 days old), animals were transferred to either 10°C or 21°C at a range of different photoperiods. 8L:16D (dashed line) was only applied in winter-born animals. Tissue collections took place when 50 days old

transcribed from linearized cDNA templates. Incorporation of 35^S-UTP (Perkin Elmer, Boston, MA, USA) was done with T7 polymerase (*Dio2* and *Dio3*) and T3 polymerase (*Tshβ*), resulting in 0.5-1.5 × 10^6 counts per minute per microliter, calculated to have 10^6 cpm/slide. All slides were fixated in paraformaldehyde, acetylated, and hybridized with radioactive probes overnight at 56°C.

Slides were washed in sodium citrate buffer the next day to remove nonspecific probe and then dehydrated in ethanol solutions, followed by air drying. The slides were exposed to an autoradiographic film (Kodak, Rochester, NY, USA) for 9 days (*Dio2* and *Dio3*) or 11 days (*Tshβ*) and developed with Carestream Kodak autoradiography GBX Developer/replenisher (P7042-1GA, Sigma) and fixer (P7167-1GA, Sigma). Films were scanned with an Epson Perfection V800 Photo scanner at 2400dpi resolution along with a calibrated optical density strip (T2115C, Stouffer Graphic Arts Equipment Co., Mishawaka, IN, USA). Analysis of integrated optical density (IOD) was done with software ImageJ, version Fuji (NIH Image, Bethesda MD, USA). The section with the highest signal was selected to represent each animal.

2.4 | Hormone analysis

Plasma testosterone levels were measured in a mouse testosterone enzyme-linked immunosorbent assay according to manufacturer's instructions (ADI-900-065; Enzo Life Sciences, New York, NY, USA). The sensitivity was 5.67 pg/mL, and the intra-assay coefficient of variation and interassay coefficient of variation were 10.8% and 9.3%, respectively.

2.5 | Calculation of critical photoperiod

Four-parameter log-logistic functions ($y = d + (c-d)/1 + (x/e)^b$) were fitted through the data using the R-package "drc,"[49] to describe the response to photoperiod as a dose-response relationship; b = slope parameter, c = minimum, d = maximum, e = 50% maximal response, where ED50 is defined as the inflexion point of the curve. Critical photoperiod was estimated by the ED50 from fitted dose-response curves. For testis mass, testosterone levels and body mass, we used a common maximum (d) within spring- and autumn experimental groups for both temperatures, but minimum (c) asymptotes were estimated for each temperature treatment. For *Tshβ*, *Dio2* and *Dio3* gene expression, the minimum (c) was set at 0. Within spring and autumn experimental groups, we set a common maximum (d) for both temperature treatments, except for *Dio3*. All fitted dose-response curve parameters can be found in Table S1. Model comparisons can be found in Table S2.

2.6 | Statistical analysis

One potential outlier for *Tshβ* were detected by boxplots, and removed from the analysis. The effects of postweaning photoperiod, ambient temperature and interactions were determined within spring and autumn experimental groups using type I two-way ANOVAs. To detect differences in growth rate between groups, we used repeated measures ANOVAs. Two-sample *t*-tests were used to determine temperature effects at specific photoperiods, and to assess changes in critical photoperiod. Statistical significance was determined at $P < .05$. All statistical analyses were performed using RStudio (version 1.2.1335),[50] and figures were generated using the R-package "ggplot2."[51] Statistic results for ANOVAs can be found in Table S3.

3 | RESULTS

3.1 | Maternal photoperiod is used to program photoperiodic gonadal responses

Exposing voles to a range of photoperiods confirms that this species shows a robust increase of testis mass, testosterone levels and body mass at long photoperiods (testis: $F_{6,70} = 39.55$, $P < .001$; testosterone: $F_{5,57} = 6.57$, $P < .001$; body mass: $F_{6,70} = 10.37$, $P < .001$; Figure 2). Fitted dose-response curves were useful to describe physiological responses to photoperiod, and allowed us to deduce ED50 (ie, critical photoperiod). In Figures 2 and 3, incomplete set of data points were available for experimental groups at 10°C. To describe dose-response curves within experimental groups, maximum response at 21°C within spring and autumn experimental groups were used, except for *Dio3*. Consequently, critical photoperiods for testosterone and Dio2 at 10°C were estimated based on extrapolated dose-response curves, and therefore have to be treated with caution.

A 1- to 2-hour shorter critical photoperiod for testis mass is observed in spring compared to autumn voles (10°C: T = 2.26, $df = 53$, $P < .03$; 21°C: T = 1.91, $df = 55$, $P < .07$; Figure 2C). Somatic growth rate is 50% higher in spring voles than in autumn voles (Figure S1 and Table S3). These findings indicate that born in winter leads to subsequent shorter critical photoperiods for reproductive activation.

3.2 | Voles at 10°C increase their gonads, but decrease testosterone levels

Lowering ambient temperature to 10°C causes an increase in testes mass (spring: $F_{1,70} = 13.18$, $P < .001$; autumn: $F_{5,50} = 12.08$, $P < .01$; Figure 2A,B). This temperature effect was primarily apparent at short photoperiods (ie, 10 and 12 hours

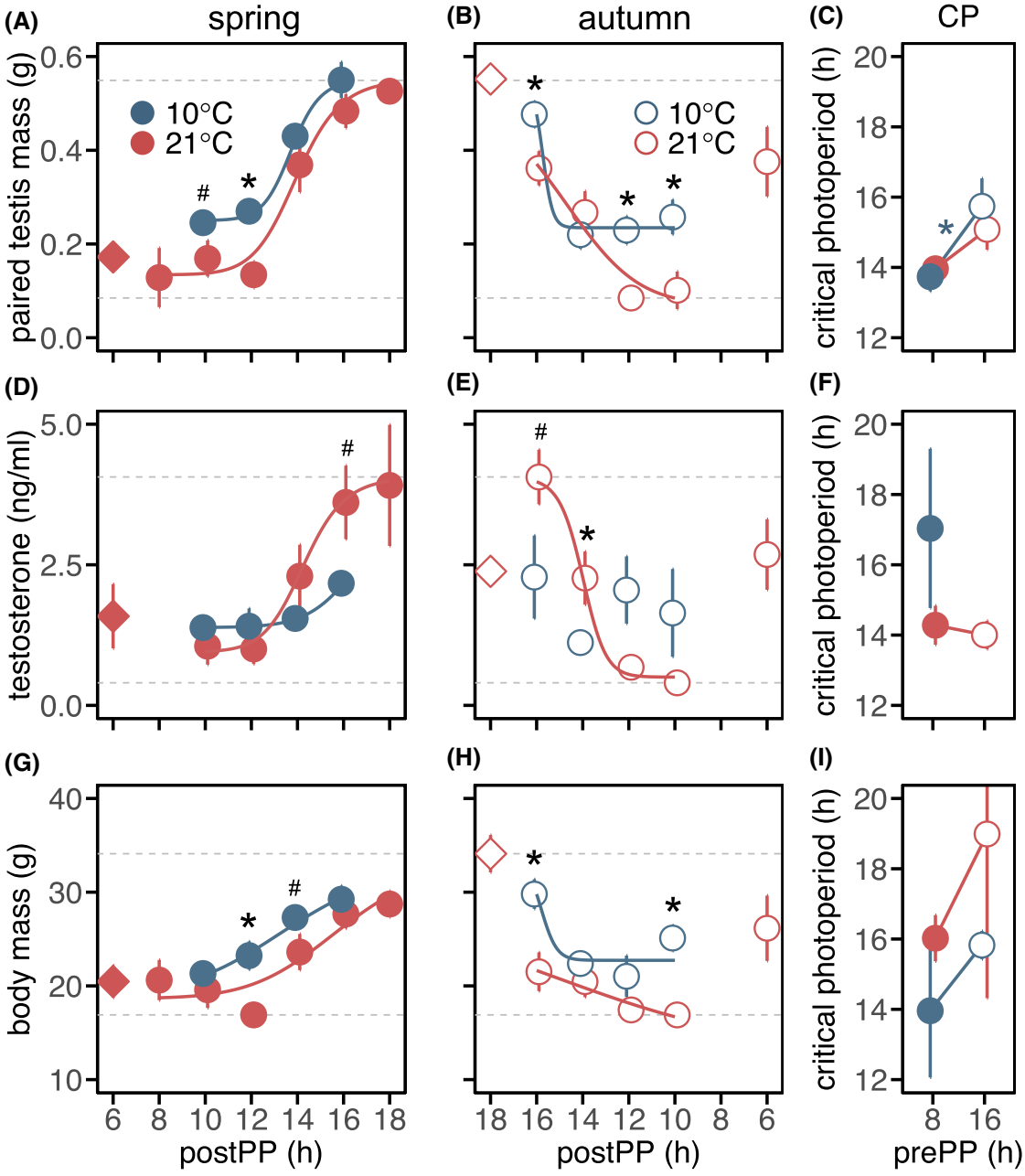

FIGURE 2 Temperature-dependent modulation of photoperiodic responses in physiological outputs. Responses to photoperiod for (A, B) paired testis mass, (D, E) plasma testosterone levels, and (G, H) body mass in 50-day-old animals for winter-born, spring (filled symbols; gestated and raised to weaning under SP) and summer-born, autumn (open symbols; gestated and raised to weaning under LP) animals, respectively, at 10°C (blue) or 21°C (red); prePP, preweaning photoperiod; postPP, postweaning photoperiod. Diamond-shaped symbols indicate photoperiodic transition in the opposite direction of round-shaped symbols. Critical photoperiods (CP) derived from fitted logistic functions are shown for (C) paired testis mass, (F) testosterone levels, and (I) body mass. Data are plotted as mean ± SEM (n = 4-8). Significant effects of contrast analyses are indicated: $^{\#}P < .1$, $^{*}P < .05$. In short, significant photoperiodic effects were found in: A, B, D, E, G, and H, significant temperature effects were found in: A, B, E, G, and H (Table S3). For dose-response curve fit parameters, we refer to Table S1; for dose-response curve model comparisons, we refer to Table S2

of light/24 hours), with twofold higher testes mass at 10°C, indicating a temperature sensitive window in early spring and late autumn (Figure S4A). Although, photoperiodic history did not change critical photoperiod for testosterone, a major lengthening of critical photoperiod was observed at 10°C (Figure 2F), resulting in a weak positive relationship between testis size and testosterone levels at 10°C (Figure S2A). Lowering temperature also accelerated somatic growth rate resulting in larger animals (spring: $F_{1,70} = 9.02$, $P < .01$; autumn: $F_{1,50} = 19.32$, $P < .001$; Figures 2G,H and S1).

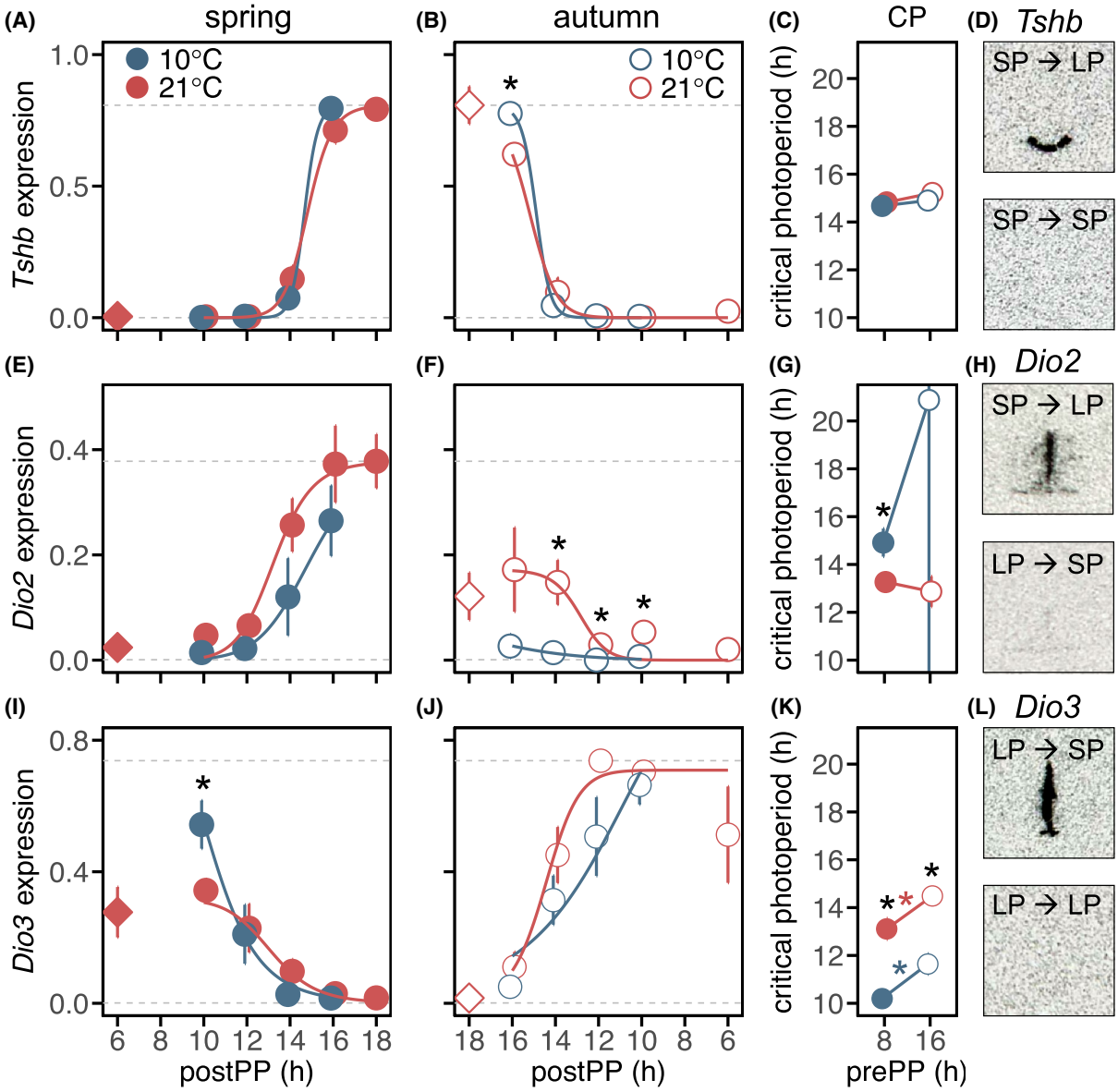

FIGURE 3 Temperature-dependent modulation of photoperiodic responses at the level of the tanycytes. Responses to photoperiod for (A, B) *Tshβ* in the pars tuberalis, (E, F) *Dio2*, and (I, J) *Dio3* in the tanycytes for winter-born, spring (filled symbols; gestated and raised to weaning under SP) and summer-born, autumn (open symbols; gestated and raised to weaning under LP) animals respectively, at 10°C (blue) or 21°C (red); prePP, preweaning photoperiod; postPP, postweaning photoperiod. Diamond-shaped symbols indicate photoperiodic transition in the opposite direction of round-shaped symbols. Images showing localization of mRNA by In situ hybridization are shown for (D) *Tshβ,* (H) *Dio2*, and (L) *Dio3* expression. Critical photoperiods (CP) derived from fitted logistic functions are shown for (C) *Tshβ*, (G) *Dio2*, and (K) *Dio3*. Data are plotted as mean ± SEM (n = 4-8). Significant effects of contrast analyses are indicated: $^{\#}P < .1$, $^{*}P < .05$. In short, significant photoperiodic effects were found in: A, B, E, I, and J, significant temperature effects were found in: E, F, and J (Table S3). For dose-response curve fit parameters we refer to Table S1; for dose-response curve model comparisons, we refer to Table S2

Overall, photoperiodic induced changes in gonadal and body mass follow and ellipse-like photoperiodic history-dependent relationship (Figure S4A,C), which is shifted upward at 10°C, indicating that temperature has an additive effect on photoperiodic-history rather than a multiplicative interaction. Photoperiodic induced changes in testosterone levels follow a temperature-dependent relationship to photoperiod, with reduced photoperiodic sensitivity at 10°C (Figure S4B).

3.3 | Photoperiodic history-dependent effects appear downstream of Tshβ in the photoperiodic axis

Melatonin binds to its receptors (MTNR1A, MT1) located in the pars tuberalis where TSHβ is produced under long photoperiods. *Tshβ* expression increases with increasing postweaning photoperiod (spring: $F_{5,39} = 233.44$, $P < .001$; autumn:

$F_{5,33} = 192.89$, $P < .001$), but is unaffected by photoperiodic-history (Figures 3A-D and S4D). TSH binds to its receptors in the tanycytes where it increases DIO2, and decreases DIO3. The observed photoperiodic responses in *Dio2* and *Dio3* expression strongly depend on photoperiodic-history: *Dio2* is enhanced in spring voles ($F_{5,81} = 3.86$, $P < .004$; Figures 3E-H and S4E), while *Dio3* is enhanced in autumn voles ($F_{5,80} = 4.30$, $P < .002$; Figures 3I-L and S4F). This results in longer critical photoperiods in autumn voles (10°C: T = 3.14, $df = 26$, $P < .005$; 21°C: T = 2.54, $df = 39$, $P < .03$; Figure 3K).

3.4 | Temperature modifies photoperiodic responses at the level of the tanycytes

Tshβ expression is unaffected by temperature (spring: $F_{1,39} = 0.01$, ns; autumn: $F_{1,33} = 1.63$, ns; Figure 3A,B), resulting in similar critical photoperiods under different conditions (Figure 3C). At 10°C, *Dio2* expression is reduced (spring: $F_{1,41} = 5.31$, $P < .05$; autumn: $F_{1,32} = 11.21$, $P < .01$; Figure 3E,F), particularly in autumn voles, where *Dio2* levels remain close to zero, even under long photoperiods. This results in longer critical photoperiods at 10°C (T = 2.40, $df = 33$, $P < .03$; Figure 3E-G). The temperature dependent change in critical photoperiod for *Dio2* is stronger in autumn than in spring voles (T = 55.52, $df = 89$, $P < .001$; Figure 3G). Temperature effects on *Dio3* expression depend on postweaning photoperiod, with slightly increased maximum expression under 10L:14D at 10°C ($F_{3,40} = 2.59$, $P < .08$; Figure 3I,J). This results in ~2 hour shorter critical photoperiods at 10°C (spring: T = 4.57, $df = 39$, $P < .001$; autumn: T = 5.17, $df = 32$, $P < .001$; Figure 3K).

Positive relationships between *Tshβ*, *Dio2* expression and testis mass, and the negative relationship between *Dio3* expression and testis mass are unaffected by temperature (Figures S2B and S3A,B,D,E). Similar positive relationships between *Tshβ* expression and testosterone, *Dio2* were observed (Figures S2C and S3C).

Overall, annual changes in *Tshβ* are primarily induced by photoperiod (Figure S4D), while photoperiodic induced changes in *Dio2* and *Dio3* follow an ellipse-like photoperiodic history-dependent relationship (Figure S4E,F), which is strongly affected by temperature for *Dio2*. The constructed annual relationship between *Tshβ* and *Dio2* confirms that *Tshβ* is either ON or OFF, and rather stable at different temperatures, while *Dio2* is completely suppressed from summer to winter at 10°C (Figure S4G). The constructed annual relationship between *Dio2* and *Dio3* shows photoperiodic-history dependence at 21°C, but not at 10°C (Figure S4I), resulting in higher *Dio3* levels at the same *Dio2* levels in warm springs.

4 | DISCUSSION

Our results confirm that ambient temperature modulates the use of photoperiod as a predictive cue for annual timing of reproduction in common voles. The melatonin-sensitive pars tuberalis was insensitive to modulation by temperature, whereas the tanycytes role in somatic and gonadal growth was sensitive to modulation by temperature. The magnitude of these temperature effects was similar in spring (ie, born early in the breeding season) and in autumn (ie, born late in the breeding season) voles. In nature, age of reproductive onset will be adjusted by the direction of photoperiodic transitions and thermal cues early in development. Although photoperiod exclusively acts as proximal predictor for seasonal metabolic preparation, temperature acts both as ultimate and proximate factor in common voles.

Physiological outputs of the photoperiodic axis (ie, testis mass, testosterone and body mass) show a positive relationship to photoperiod (Figure 2), as described in hamsters.[52,53] Gene expression patterns in the pars tuberalis (ie, *Tshβ*) and tanycytes (*Dio2*, *Dio3*) also follow a positive relationship to photoperiod (Figure 3), which supports previous findings confirming photoperiodic responsiveness of those genes in common voles.[44,45]

Here we show that photoperiodic relationships can be described by dose-response curves, from which critical photoperiods can be derived as inflexion points, ED50. Whether photoperiod can be seen as a dose is debatable, since it has been shown that it is not the photoperiodic length per se, but rather the circadian phase at which light is perceived that determines melatonin suppression leading to photoperiodic responses.[39,40] Critical photoperiods for gonadal responses have been described before in hamsters,[53-55] and at the level of the pars tuberalis and tanycytes in Soay sheep.[56,57]

The critical photoperiod for acceleration of gonadal development in voles gestated on SP is markedly shorter than for arrest of gonadal development in voles gestated on LP (Figure 2C). This difference may lead to accelerated reproductive development when born in spring, to deliver offspring in summer, when there are sufficient food resources for pregnancy, lactation and pup growth. On the other hand, long critical photoperiods in autumn voles may delay reproductive onset until next spring. In autumn animals, biphasic photoperiodic responses have been observed in physiological measures (Figure 2B,E,H), but this is not reflected in hypothalamic gene expression patterns (Figure 3B,F,J). Bimodal curves are also observed in prolactin levels and ovarian cyclicity in sheep, and suggests a limited photoperiodic window of the long day response.[58] At 53°N latitude, from which our *M. arvalis* lab population originates, civil twilight-based photoperiod varies annually between 8.92 and 18.77 hours.[59]

Therefore, the extreme photoperiods of 6:18 and 18:6 hours used in the current study are not or only briefly experienced by our voles in the field. Limited capacity of adaptive responses to these extreme photoperiods may therefore explain the high physiological responses at 6:18 and 18:6 hours and their deviation from the expected dose-response-curve relationships.

Photoperiodic history-dependent effects appear downstream of *Tshβ* in the photoperiodic-axis (Figures 2, 3 and S4), which previously has been confirmed in Siberian hamsters,[11] where increased responses to intermediate photoperiod when born under SP were described as increased sensitivity to photoperiod. This is understandable as the photoperiodic response can be described as a dose-response relationship, where the inflection point has shifted to shorter photoperiods. Hence, indicating increased sensitivity to photoperiod, and therefore increased responses to intermediate photoperiods. However, full dose-response curves are required to demonstrate changes in sensitivity. Our data describe full dose-response curves, and show that indeed the sensitivity to photoperiod has increased in animals born under SP, which explained increased responses to intermediate photoperiods. Increased *Tshr* expression in the tanycytes early in development of vole and hamsters raised under constant SP,[11,45] may lead to increased TSH sensitivity, which may therefore provide an explanation for elevated *Dio2*, and reduced *Dio3* levels in spring animals compared to autumn animals (Figure 3).

The greatest part of the dose-response curve for *Tshβ* is not affect by temperature (Figure 3A,B), but 1 outlier, with high *Tshβ* levels at short photoperiods have been removed from the data set. Interestingly, this outlier belonged to the 10°C experimental groups, indicating that photoperiodic non-responsiveness, which is observed to vary among individuals within populations,[60,61] can be triggered by low ambient temperature.

The finding that testis mass increases at 10°C, primarily under short photoperiods (Figure 2A,B), suggests that early spring and late autumn are temperature sensitive windows for gonadal development. Increasing photoperiod in combination with 10°C and ad libitum food conditions may be a predictor for nearly spring arrival. This interpretation is confirmed by annual temperature patterns at 53°N latitude (were our laboratory colony originates from), which shows that 10°C at increasing photoperiod appears in late April.[59] Our findings are inconsistent with previous studies in hamsters and other vole species, showing decreased gonadal size at 5°C under short and intermediate photoperiods.[20,54,62] This inconsistency may be explained by the fact that at 5°C ambient temperature grass growth is not initiated yet.[63-65] However, species differences in temperature sensitivity cannot be excluded. Bronson and Pryor showed that optimal temperatures for breeding in deer mice greatly varies between latitude of origin.[66] In addition, house mice reproduce in the laboratory at −6°C ambient temperature if food is available in excess throughout the day.[66] Applying a broader range of ambient temperatures under different photoperiodic transitions may reveal an optimal temperature window for reproductive onset and offset in different species.

Testis mass and testosterone levels correlate well under short photoperiods, but under longer photoperiods higher testes mass corresponds to suppressed testosterone levels at 10°C (Figures 2D,E and S2A). Testis development is a time-consuming process, but will rapidly develop in voles born in a cold spring, leading to fully developed testes later in spring when temperatures are rising and testosterone production can be quickly elevated. Increased spermatogenesis due to the presence of testosterone in the testis[68] may therefore lead to quick adaptive responses when spring arrives. Based on annual photoperiodic changes at 53°N latitude, a 14-day earlier onset of testes development (above 50% response) is predicted at 10°C, perhaps leading to a slightly longer seasonal period of large testes when temperatures are low (Figure 4A). On the other hand, testosterone production (above 50% response) may start 2 months later at 10°C, perhaps leading to a dramatic delay and shortening of the breeding season at lower ambient temperatures (Figure 4A).

To adapt annual timing of reproduction to a warming environment due to climate change, mammals need to either change critical photoperiod or eliminate photoperiodic control.[15] Previous selection experiments in short-lived rodents showed that within a single generation, the degree of photoperiodic responsiveness can be highly changed.[69-71] The finding that thermal cues can overrule photoperiodic cues along with short life expectancy and short reproductive cycles, suggests that common voles will relatively quickly ecologically adapt to climate change. Although, we experimentally assessed multiple interactions between different photoperiod and temperature conditions, we do not have data for the complete landscape of (long-term) photoperiodic transitions in relation to all different temperature combinations that occur in the field. Translating these findings to natural conditions is therefore complicated, and should be interpreted with caution. Furthermore, in our experiments, food was available ad libitum, causing voles to be able to compensate for thermoregulatory costs by increasing food intake when temperatures are low. Whether ambient temperature has similar effects on the photoperiodic axis when food is scarce, remains to be experimentally assessed. Furthermore, in this study, we assessed temperature effects on the male reproductive system, while the impact of temperature on the female reproductive system may be of greater importance, since pregnancy and lactation are energy-consuming processes.[67] In addition, spermatogenesis is a more continuous process than ovulation, and therefore the temperature effects on female reproduction may be more critical in affecting fertility. Future studies need

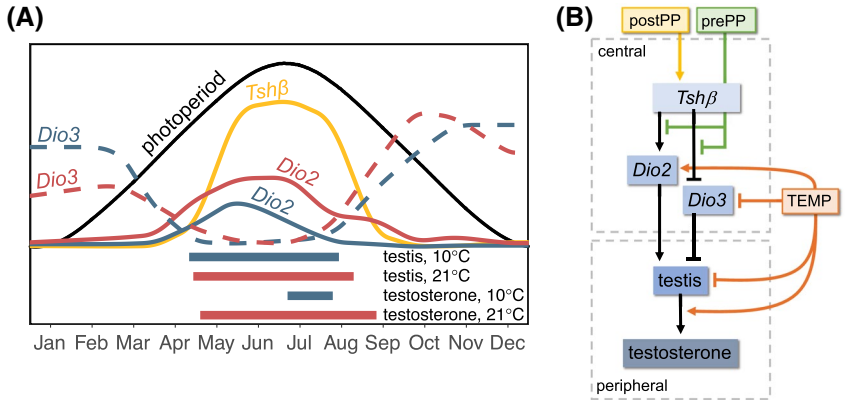

FIGURE 4 Photoperiod and temperature affect the photoperiodic neuroendocrine system. A, Photoperiodic history and temperature-dependent annual fluctuations are shown for: photoperiod (black line), *Tshβ* (yellow line), *Dio2* at 10°C (solid blue line), *Dio2* at 21°C (solid red line), *Dio3* at 10°C (dashed blue line), and *Dio3* at 21°C (dashed red line). Period when testes mass and testosterone levels are above 50% response at 10°C and 21°C is depicted below the graph. B, The scheme shows the effects of postweaning photoperiod (postPP), pre-weaning photoperiod (prePP) and ambient temperature (temp) at different levels central and peripheral in the photoperiodic neuroendocrine system

to assess whether male and female voles respond to the same environmental cues to synchronize their reproductive season.

Temperature effects at the level of the tanycytes are much more explicit, with *Dio2* being strongly downregulated and *Dio3* being slightly upregulated at 10°C in spring voles, and slightly downregulated at 10°C in autumn voles (Figures 3 and S4E,F). Although TSH generally leads to increased *Dio2* and decreased *Dio3*,[37,43,72] the absence of temperature effects in *Tshβ* is not reflected in *Dio2*/*Dio3* expression, suggesting that factors other than TSH can affect *Dio2* expression in the tanycytes. The *Dio2* ~ *Dio3* relationship has previously been shown to be mutually exclusive in common voles exposed to constant photoperiods.[44] However, this effect seems to be less strong at 21°C in relation to photoperiodic-history, where *Dio3* remains high in warm springs while *Dio2* is rising at both temperatures (Figure S4I). Higher *Dio3* levels in warm springs may result in reduced T_3 levels, which ultimately suppress gonadal development. This may provide an explanation for voles having small testes and low testosterone levels under short photoperiods at 21°C (Figures 2A,D and S4A,B).

At 21°C, *Dio2* and testosterone production are controlled by photoperiod, whereas at low temperature, photoperiodic control is limited and suppression takes place. The long critical photoperiods for *Dio2* and testosterone at low temperature, indicate that thermal cues can overrule photoperiodic signals to control seasonal reproduction, which implies opportunistic acting based on metabolic conditions. However, testis growth is under photoperiodic control under all conditions. This observation shows that different outputs of the photoperiodic system can vary in sensitivity to temperature modulation of photoperiodic responses.

Under long photoperiods, *Dio3* is close to zero at both temperatures, while *Dio2* is higher at 21°C (Figures 3E, F, I, J and S4E, F, I). This may result in high central T_3 levels, which is reflected in high testosterone levels at 21°C under LP (Figure 2D and S4B). The lack of a simple relationship between testis size and testosterone at 10°C (Figure S2A) implies that testosterone production can be regulated independent of testis size per se. One possible mechanism involves FSH which increases sertoli cell division rate,[73] and selectively restores spermatogenesis despite low testosterone levels.[74] Sustained negative steroid feedback on the hypothalamus and pituitary, regulating GnRH and FSH/LH secretion respectively might be changed by temperature.[75] This may lead to increased FSH levels, leading to accelerated testes growth and spermatogenesis, and low LH levels leading to suppressed testosterone production, when temperatures are low.

Another possible underlying mechanism involves T_3. In quail, a long-day breeding bird, low ambient temperature stimulates testicular regression, induced by T_3 induction by increased DIO2 in liver.[76] In mammals, cold exposure leads to increased DIO2 levels in brown adipose tissue (BAT), which in turn produces T_3, leading to increased circulating T_3.[77-79] Brandt's voles (*Lasiopodomys brandtii*) indeed have high serum T_3 levels when exposed to cold.[80] Although T_3 stimulates testicular regression in birds, T_3 has dual functions in promoting amphibian metamorphoses: epidermal differentiation of head and body and apoptosis of the tale.[81] Therefore, plasma T_3 may induce differential responses on Sertoli and Leydig cells,[82] leading to a lack of relationship between testis size and testosterone production under cold exposure. It would also be important to study potential mechanisms involved in temperature-induced modifications of photoperiodic central T_3 responses. One potential mechanisms is the Kiss-GnRH neuronal system located in the preoptic-area of the hypothalamus which is involved in temperature regulation.[24,25]

Altogether our findings show that photoperiodic responses in common voles are plastic, and can be modified in response to photoperiodic history and ambient temperature.

Thus, common voles show some degree of opportunism in their annual reproductive strategy. We show that photoperiodic temperature and history-dependent effects appear downstream of *Tshβ* in the photoperiodic axis (Figure 4B). Ambient temperature modifies tanycytic *Dio2*/*Dio3* relationship patterns, which is reflected in physiological responses. Our observations confirm that common voles use a photoperiodic breeding strategy, which can be modified by temperature. Because the vole is an essential herbivorous species in terrestrial ecosystems,[83] defining the mechanisms underlying temperature effects on the reproductive axis will be important for a better understanding of how annual cycling environmental cues impact reproductive function, plasticity in life-history strategies, and population cycle dynamics in vole populations in a changing climate.

ACKNOWLEDGMENTS

We thank R. Schepers for his valuable help in tissue collections and animal care, Dr. H. Dardente for providing the probes for *in situ* hybridization and Prof. Dr. M.P. Gerkema for establishing the common vole colony at the University of Groningen. This work was funded by the Adaptive Life program of the University of Groningen (B050216 to LvR, RTMR, and LdW and RAH), and by the Arctic University of Norway (Universitetet i Tromsø to JvD, DA, and DGH).

CONFLICT OF INTEREST

The authors declare no conflicting interest.

AUTHOR CONTRIBUTIONS

L. van Rosmalen, D.G. Hazlerigg, and R.A. Hut designed the experiments; L. van Rosmalen, J. van Dalum, D. Appenroth, R.T.M. Roodenrijs, L. de Wit, and R.A. Hut conducted the experiments; L. van Rosmalen and J. van Dalum analyzed the data; L. van Rosmalen, D.G. Hazlerigg, and R.A. Hut wrote the paper; all authors read and commented on the paper.

REFERENCES

1. Negus NC, Berger PJ, Forslund LG. Reproductive strategy of *Microtus montanus*. *J Mammal*. 1977;58(3):347-353.
2. Negus NC, Berger PJ, Pinter AJ. Phenotypic plasticity of the montane vole (*Microtus montanus*) in unpredictable environments. *Can J Zool*. 1992;70(11):2121-2124. https://doi.org/10.1139/z92-285
3. Negus NC, Berger PJ, Brown BW. Microtine population dynamics in a predictable environment. *Can J Zool*. 1986;64(3):785-792. https://doi.org/10.1139/z86-117
4. Hoffmann K. Effects of short photoperiods on puberty, growth and moult in the Djungarian hamster (*Phodopus sungorus*). *J Reprod Fertil*. 1973;54:29-35.
5. Horton TH. Growth and reproductive is affected development by the prenatal of male *Microtus montanus* photoperiod. *Biol Reprod*. 1984;504:499-504.
6. Stetson MH, Elliott JA, Goldman BD. Maternal transfer of photoperiodic information influences the photoperiodic response of prepubertal Djungarian hamsters (*Phodopus sungorus*). *Biol Reprod*. 1986;34(4):664-669. https://doi.org/10.1095/biolreprod34.4.664
7. Yellon SM, Goldman BD. Photoperiod control of reproductive development in the male Djungarian hamster (*Phodopus sungorus*). *Endocrinology*. 1984;114(2):664-670.
8. Horton TH. Cross-fostering of voles demonstrates in utero effect of photoperiod. *Biol Reprod*. 1985;33(4):934-939. https://doi.org/10.1095/biolreprod33.4.934
9. Horton TH, Stetson MH. Maternal transfer of photoperiodic information in rodents. *Anim Reprod Sci*. 1992;30(1-3):29-44. https://doi.org/10.1016/0378-4320(92)90004-W
10. Prendergast BJ, Gorman MR, Zucker I. Establishment and persistence of photoperiodic memory in hamsters. *Proc Natl Acad Sci*. 2000;97(10):5586-5591. https://doi.org/10.1073/pnas.100098597
11. Sáenz de Miera C, Bothorel B, Jaeger C, Simonneaux V, Hazlerigg D. Maternal photoperiod programs hypothalamic thyroid status via the fetal pituitary gland. *Proc Natl Acad Sci*. 2017;114(31):8408-8413. https://doi.org/10.1073/pnas.1702943114
12. Sáenz De Miera C. Maternal photoperiodic programming enlightens the internal regulation of thyroid-hormone deiodinases in tanycytes. *J Neuroendocrinol*. 2019;31(1):12679. https://doi.org/10.1111/jne.12679
13. Van DJ, Melum VJ, Wood SH, Hazlerigg DG. Maternal photoperiodic programming: melatonin and seasonal synchronization before birth. *Front Endocrinol (Lausanne)*. 2020;10(January):1-7. https://doi.org/10.3389/fendo.2019.00901
14. Bronson FH *Mammalian Reproductive Biology*. Chicago, IL: University of Chicago Press; 1989. https://doi.org/10.1016/0306-4530(90)90082-k
15. Bronson FH. Climate change and seasonal reproduction in mammals. *Philos Trans R Soc B Biol Sci*. 2009;364(1534):3331-3340. https://doi.org/10.1098/rstb.2009.0140
16. Negus NC, Berger PJ. Experimental triggering of reproduction in a natural population of *Microtus montanus*. *Science (80-)*. 1977;196(4295):1230-1231.
17. Sanders EH, Gardner PD, Berger PJ, Negus NC. 6-methoxybenzoxazolinone: a plant derivative that stimulates reproduction in *Microtus montanus*. *Science (80-)*. 1981;214(4216):67-69.
18. Larkin JE, Freeman DA, Zucker I. Low ambient temperature accelerates short-day responses in Siberian hamsters by altering responsiveness to melatonin. *J Biol Rhythms*. 2001;16(1):76-86. https://doi.org/10.1177/074873040101600109
19. Kriegsfeld LJ, Trasy AG, Nelson RJ. Temperature and photoperiod interact to affect reproduction and GnRH synthesis in male prairie voles. *J Neuroendocrinol*. 2000;12(6):553-558. https://doi.org/10.1046/j.1365-2826.2000.00485.x
20. Nelson RJ, Frank D, Smale L, Willoughby SB. Photoperiod and temperature affect reproductive and nonreproductive functions in male prairie voles (*Microtus ochrogaster*). *Biol Reprod*. 1989;40(3):481-485. https://doi.org/10.1095/biolreprod40.3.481
21. Steinlechner S, Puchalski W. *Mechanisms for Seasonal Control of Reproduction in Small Mammals*. Heidelberg: Springer-Verlag Berlin; 2003.
22. Nelson RJ, Dark J, Zucker I. Influence of photoperiod, nutrition and water availability on reproduction of male California voles (*Microtus californicus*). *J Reprod Fertil*. 1983;69:473-477. https://doi.org/10.1530/jrf.0.0690473
23. Simons MJP, Reimert I, van der Vinne V, et al. Ambient temperature shapes reproductive output during pregnancy and lactation

in the common vole (*Microtus arvalis*): a test of the heat dissipation limit theory. *J Exp Biol*. 2011;214(1):38-49. https://doi.org/10.1242/jeb.044230

24. Caro SP, Schaper SV, Hut RA, Ball GF, Visser ME. The case of the missing mechanism: how does temperature influence seasonal timing in endotherms? *PLoS Biol*. 2013;11(4):e1001517. https://doi.org/10.1371/journal.pbio.1001517
25. Hut RA, Dardente H, Riede SJ. Seasonal timing: how does a hibernator know when to stop hibernating? *Curr Biol*. 2014;24(13):602-605. https://doi.org/10.1016/j.cub.2014.05.061
26. Dardente H, Wood S, Ebling F, Sáenz de Miera C. An integrative view of mammalian seasonal neuroendocrinology. *J Neuroendocrinol*. 2018;31(5):e12729. https://doi.org/10.1111/jne.12729
27. Nakane Y, Yoshimura T. Photoperiodic regulation of reproduction in vertebrates. *Annu Rev Anim Biosci*. 2019;7:173-194. https://doi.org/10.1146/annurev-animal-020518-115216Copyright
28. Klein DC, Weller JL. Indole metabolism in the pineal gland: a circadian rhythm in N-acetyltransferase. *Science (80-)*. 1970;169(3950):1093-1095.
29. Williams LM, Morgan PJ. Demonstration of melatonin-binding sites on the pars tuberalis of the rat. *J Endocrinol*. 1988;119(1):1-3.
30. Dardente H, Klosen P, Pévet P, Masson-Pévet M. MT1 melatonin receptor mRNA expressing cells in the pars tuberalis of the European hamster: effect of photoperiod. *J Neuroendocrinol*. 2003;15(8):778-786. https://doi.org/10.1046/j.1365-2826.2003.01060.x
31. Morgan PJ, Barrett P, Howell HE, Helliwell R. Melatonin receptors: localization, molecular, pharmacology and physiological significance. *Neurochem Int*. 1994;24(2):101-146.
32. Yasuo S, Yoshimura T, Ebihara S, Korf HW. Melatonin transmits photoperiodic signals through the MT1 melatonin receptor. *J Neurosci*. 2009;29(9):2885-2889. https://doi.org/10.1523/JNEUROSCI.0145-09.2009
33. Hazlerigg D, Loudon A. New insights into ancient seasonal life timers. *Curr Biol*. 2008;18(17):795-804. https://doi.org/10.1016/j.cub.2008.07.040
34. Magner JA. Thyroid-stimulating hormone: biosynthesis, cell biology, and bioactivity. *Endocr Rev*. 1990;11(2):354-385.
35. Simonneaux V. A Kiss to drive rhythms in reproduction. *Eur J Neurosci*. 2020;51(1):509-530. https://doi.org/10.1111/ejn.14287
36. Hut RA. Photoperiodism: shall EYA compare thee to a summers day? *Curr Biol*. 2011;21(1):R22-R25. https://doi.org/10.1016/j.cub.2010.11.060
37. Nakao N, Ono H, Yamamura T, et al. Thyrotrophin in the pars tuberalis triggers photoperiodic response. *Nature*. 2008;452(7185):317-322. https://doi.org/10.1038/nature06738
38. Ono H, Hoshino Y, Yasuo S, et al. Involvement of thyrotropin in photoperiodic signal transduction in mice. *PNAS*. 2008;105(47):18238-18242. https://doi.org/10.1073/pnas.0808952105
39. Dardente H, Wyse CA, Birnie MJ, et al. A molecular switch for photoperiod responsiveness in mammals. *Curr Biol*. 2010;20(24):2193-2198. https://doi.org/10.1016/j.cub.2010.10.048
40. Masumoto K-H, Ukai-Tadenuma M, Kasukawa T, et al. Acute induction of Eya3 by late-night light stimulation triggers TSHβ expression in photoperiodism. *Curr Biol*. 2010;20(24):2199-2206. https://doi.org/10.1016/j.cub.2010.11.038
41. Sáenz de Miera C, Monecke S, Bartzen-Sprauer J, et al. A circannual clock drives expression of genes central for seasonal reproduction. *Curr Biol*. 2014;24(13):1500-1506. https://doi.org/10.1016/j.cub.2014.05.024
42. Wood S, Christian H, Miedzinska K, et al. Binary switching of calendar cells in the pituitary defines the phase of the circannual cycle in mammals. *Curr Biol*. 2015;25(20):2651-2662. https://doi.org/10.1016/j.cub.2015.09.014
43. Hanon EA, Lincoln GA, Fustin J-M, et al. Ancestral TSH mechanism signals summer in a photoperiodic mammal. *Curr Biol*. 2008;18(15):1147-1152. https://doi.org/10.1016/j.cub.2008.06.076
44. Król E, Douglas A, Dardente H, et al. Strong pituitary and hypothalamic responses to photoperiod but not to 6-methoxy-2-benzoxazolinone in female common voles (*Microtus arvalis*). *Gen Comp Endocrinol*. 2012;179(2):289-295. https://doi.org/10.1016/j.ygcen.2012.09.004
45. van Rosmalen L, van Dalum J, Hazlerigg DG, Hut RA. Gonads or body? differences in gonadal and somatic photoperiodic growth response in two vole species. *J Exp Biol*. 2020;223:jeb.230987. https://doi.org/10.1242/jeb.230987
46. Gerkema MP, Daan S, Wilbrink M, Hop MW, Van Der Leest F. Phase control of ultradian feeding rhythms in the common vole (*Microtus arvalis*): the roles of light and the circadian system. *J Biol Rhythms*. 1993;8(2):151-171. https://doi.org/10.1177/074873049300800205
47. Appenroth D, Melum VJ, West AC, Dardente H, Hazlerigg DG, Wagner GC. Photoperiodic induction without light-mediated circadian entrainment in a High Arctic resident bird. *J Exp Biol*. 2020;223(16):jeb220699. https://doi.org/10.1242/jeb.220699
48. Lomet D, Cognié J, Chesneau D, Dubois E, Hazlerigg D, Dardente H. The impact of thyroid hormone in seasonal breeding has a restricted transcriptional signature. *Cell Mol Life Sci*. 2018;75(5):905-919. https://doi.org/10.1007/s00018-017-2667-x
49. Ritz C, Baty F, Streibig JC, Gerhard D. Dose-response analysis using R. *PLoS One*. 2015;10(12):1-13. https://doi.org/10.1371/journal.pone.0146021
50. Team RC. *R: A Language and Environment for Statistical Computing*. Vienna, Austria: R Found Stat Comput. Published online 2013. https://doi.org/10.1108/eb003648
51. Wickham H. *Ggplot2: Elegant Graphics for Data Analysis*. New York: Springer-Verlag; 2016. https://doi.org/10.1007/978-3-319-24277-4_1
52. Elliott JA. Circadian rhythms and photoperiodic time measurement in mammals. *Fed Proc*. 1976;35(12):2339-2346.
53. Gaston S, Menaker M. Photoperiodic control of hamster testis. *Science (80-)*. 1967;158(3803):925-928.
54. Steinlechner S, Stieglitz A, Ruf T, Heldmaier G, Reiter RJ. Integration of environmental signals by the pineal gland and its significance for seasonality in small mammals. In: Fraschini F, Reiter RJ, eds. *Role of Melatonin and Pineal Peptides in Neuroimmunomodulation*. New York: Plenum Press; 1991:159-163.
55. Hoffmann K. The critical photoperiod in the Djungarian hamster *Phodopus sungorus*. In: Aschoff J, Daan S, Groos G, eds. *Vertebrate Circadian Systems*. Heidelberg: Springer-Verlag Berlin; 1982:297-304.
56. Hazlerigg D, Lomet D, Lincoln G, Dardente H. Neuroendocrine correlates of the critical day length response in the Soay sheep. *J Neuroendocrinol*. 2018;30(9):e12631. https://doi.org/10.1111/jne.12631
57. Dardente H, Lomet D, Chesneau D, Pellicer-Rubio MT, Hazlerigg D. Discontinuity in the molecular neuroendocrine response to increasing daylengths in Ile-de-France ewes: is transient Dio2

induction a key feature of circannual timing? *J Neuroendocrinol*. 2019;31(8):1-10. https://doi.org/10.1111/jne.12775
58. Wagner GC, Johnston JD, Clarke IJ, Lincoln GA, Hazlerigg DG. Redefining the limits of day length responsiveness in a seasonal mammal. *Endocrinology*. 2008;149(1):32-39. https://doi.org/10.1210/en.2007-0658
59. Hut RA, Paolucci S, Dor R, Kyriacou CP, Daan S. Latitudinal clines: an evolutionary view on biological rhythms. *Proc R Soc B Biol Sci*. 2013;280(1765):1-9. https://doi.org/10.1098/rspb.2013.0433
60. Nelson RJ. Photoperiod-nonresponsive morphs: a possible variable in *Microtine* population-density fluctuations. *Univ Chicago Press*. 1987;130(3):350-369.
61. Kliman RM, Lynch RG. Evidence for genetic variation in the occurrence of the photoresponse of the Djungarian hamster, Phodopus sungorus. *J Biol Rhythms*. 1992;7(2):161-173.
62. Baker JR, Ranson RM. Factors affecting the breeding of the field mouse (*Microtus agrestis*). Part II. temperature and food. *Proc R Soc B Biol Sci*. 1932;112(774):39-46.
63. Peacock JM. Temperature and leaf growth in four grass species. *J Appl Ecol*. 1976;13(1):225-232.
64. Peacock JM. Temperature and leaf growth in *Lolium perenne*. II. The site of temperature perception. *J Appl Ecol*. 1975;12(1):115-123.
65. Cooper JP. Climatic variation in forage grasses. I. Leaf development in climatic races of *Lolium* and *Dactylis*. *J Appl Ecol*. 1964;1(1):45-61. https://doi.org/10.2307/2401588
66. Bronson FH, Pryor S. Ambient temperature and reproductive success in rodents living at different latitudes. *Biol Reprod*. 1983;29(1):72-80.
67. Speakman JR. The physiological costs of reproduction in small mammals. *Philos Trans R Soc B Biol Sci*. 2008;363(1490):375-398. https://doi.org/10.1098/rstb.2007.2145
68. Walker WH. Testosterone signaling and the regulation of spermatogenesis. *Spermatogenesis*. 2011;1(2):116-120. https://doi.org/10.4161/spmg.1.2.16956
69. Heideman PD, Bronson FH. Characteristics of a genetic polymorphism for reproductive photoresponsiveness in the white-footed mouse (*Peromyscus leucopus*). *Biol Reprod*. 1991;44:1189-1196.
70. Goldman SL, Dhandapani K, Goldman BD. Genetic and environmental influences on short-day responsiveness in Siberian hamsters (*Phodopus sungorus*). *J Biol Rhythms*. 2000;15(5):417-428. https://doi.org/10.1177/074873000129001503
71. Spears N, Clark JR. Selection in field voles (*Microtus agrestis*) for gonadal growth under short photoperiods. *J Anim Ecol*. 1988;57(1):61-70.
72. Guerra M, Blázquez JL, Peruzzo B, et al. Cell organization of the rat pars tuberalis. Evidence for open communication between pars tuberalis cells, cerebrospinal fluid and tanycytes. *Cell Tissue Res*. 2010;339(2):359–381. https://doi.org/10.1007/s00441-009-0885-8
73. Meachem SJ, McLachlan RI, de Kretser DM, Robertson DM, Wreford NG. Neonatal exposure of rats to recombinant follicle stimulating hormone increases adult Sertoli and spermatogenic cell numbers. *Biol Reprod*. 1996;54(1):36-44. https://doi.org/10.1095/biolreprod54.1.36
74. Lerchl A, Sotiriadou S, Behre HM, et al. Restoration of spermatogenesis by follicle-stimulating hormone despite low Intratesticular testosterone in photoinhibited hypogonadotropic Djungarian hamsters (*Phodopus sungorus*). *Biol Reprod*. 1993;49(5):1108-1116.
75. Gupta D. Hypothalamic control of the mammalian sexual maturation. *Padiatr Padol*. 1977;5:83-102.
76. Ikegami K, Atsumi Y, Yorinaga E, et al. Low temperature-induced circulating triiodothyronine accelerates seasonal testicular regression. *Endocrinology*. 2015;156(2):647-659. https://doi.org/10.1210/en.2014-1741
77. Silva JE, Larsen PR. Potential of brown adipose tissue type II thyroxine 5'-deiodinase as a local and systemic source of triiodothyronine in rats. *J Clin Invest*. 1985;76(6):2296-2305. https://doi.org/10.1172/JCI112239
78. de Jesus LA, Carvalho SD, Ribeiro MO, et al. The type 2 iodothyronine deiodinase is essential for adaptive thermogenesis in brown adipose tissue. *J Clin Invest*. 2001;108(9):1379-1385. https://doi.org/10.1172/JCI200113803
79. Lowell BB, Spiegelman BM. Towards a molecular understanding of adaptive thermogenesis. *Nature*. 2000;404(6778):652-660. https://doi.org/10.1038/35007527
80. Zhang Q, Lin Y, Zhang XY, Wang DH. Cold exposure inhibits hypothalamic Kiss-1 gene expression, serum leptin concentration, and delays reproductive development in male Brandt's vole (*Lasiopodomys brandtii*). *Int J Biometeorol*. 2015;59(6):679-691. https://doi.org/10.1007/s00484-014-0879-4
81. Denver RJ. Neuroendocrinology of amphibian metamorphosis. In: Shi Y-B, ed. *Current Topics in Developmental Biology*, 1st edn, vol. 103. Burlington, VT: Elsevier Inc; 2013:195-227. https://doi.org/10.1016/B978-0-12-385979-2.00007-1
82. Wagner MS, Wajner SM, Maia AL. The role of thyroid hormone in testicular development and function. *J Endocrinol*. 2008;199(3):351-365. https://doi.org/10.1677/JOE-08-0218
83. Bakker E, Olff H, Boekhoff M, Gleighman J, Berendse F. Impact of herbivores on nitrogen cycling. *Oecologia*. 2004;138(1):91-101. https://doi.org/10.1007/s00442-003-1402-5

SUPPORTING INFORMATION

Additional Supporting Information may be found online in the Supporting Information section.

How to cite this article: van Rosmalen L, van Dalum J, Appenroth D, et al. Mechanisms of temperature modulation in mammalian seasonal timing. *The FASEB Journal*. 2021;35:e21605. https://doi.org/10.1096/fj.202100162R